Supporting Information

Microwave-assisted synthesis of ZIF-9@xGO composites as cooperative electrocatalysts for electro-oxidation of benzyl alcohols coupled with H_2 production

Sayantan Chongdar,[1,ǂ] Anirban Ghosh,[1,ǂ] Rajaram Bal[2,3] and Asim Bhaumik[1,*]

Experimental Section

Chemicals: Graphite powder (Sigma-Aldrich), sodium nitrate ($NaNO_3$, Loba Chemie), cobalt nitrate hexahydrate (Co $(NO_3)_2.6H_2O$, 98%, Sigma-Aldrich), benzimidazole (Bim, Loba Chemie), *N,N*-dimethylformamide (DMF, 99.8%, Rankem), nitric acid (HNO_3, 69.70%, Rankem), potassium hydroxide (KOH, Rankem), benzyl alcohol anhydrous (99.8%, Spectrochem), 4-fluorobenzyl alcohol (Sigma-Aldrich), 4-methylbenzyl alcohol (Sigma-Aldrich), 4-bromobenzyl alcohol (Sigma-Aldrich), 4-methoxybenzyl alcohol (Sigma-Aldrich), 4-nitrobenzyl alcohol (Sigma-Aldrich), 3-chlorobenzyl alcohol (Sigma-Aldrich), 3-fluorobenzyl alcohol (Sigma-Aldrich), furfuryl alcohol (Sigma-Aldrich), cinnamyl alcohol (Sigma-Aldrich), nafion perfluorinated resin solution (Sigma-Aldrich), nickel foam (Sigma-Aldrich), isopropyl alcohol (Rankem). All solvents were used without further purification.

Materials Characterization: The single crystals of ZIF-9 was diffracted using Bruker D8 VENTURE microfocus diffractometer equipped with a PHOTON II detector using Mo K_α (λ = 0.0709 nm) radiation. Anton Paar Microwave 300 was used to synthesize ZIF-9 and ZIF-9@xGO composites. The bulk phase was characterized *via* powder X-ray diffraction (PXRD) using Bruker AXS D8 Advanced SWAX diffractometer (Cu K_α, λ = 0.15406 nm). For raman spectroscopy J-Y Horiba (Model - T64000) equipped with 1800 grooves/mm gratings was used. The samples were excited with 532 nm wavelength laser from DPSS Nd:YAG laser. All FTIR data were recorded using PerkinElmer Spectrum 100 Fourier-transform infrared (FTIR) spectrometer. The diffuse reflectance spectra (DRS) were obtained using Shimadzu UV-2401PC UV-Vis spectrophotometer (barium sulfate, $BaSO_4$, as the reflectance standard). To examine the thermal stability TGA profile under continuous air flow, TA-SDQ Q-600 thermal analyser was utilized. The Brunauer-Emmett-Teller (BET) surface area measurement at 77 K of the samples were performed using iSorbHP-100 gas sorption analyzer of Anton Paar QuntaTec, USA (Serial no. 1050020741). X-ray photoelectron spectroscopic (XPS) data were collected using an Omicron Nanotechnology XPS 0571 spectrometer. JEM 2100 (JEOL, Japan) high resolution transmission electron microscope (HRTEM) and JEOL JSM-7500F FESEM were used for the microscopic analysis. Electrochemical measurements were carried out on Metrohm Autolab PGSTAT204 electrochemical workstation (Serial no. AUT51787, Netherlands). All of the electrochemical data were presented without iR correction. Using Bruker Avance Neo 600 we recorded the ^1H and ^{13}C NMR data. CS-5800D Centurion

Scientific Gas Chromatograph (GC) was used to determine the evolved H_2 gas. GC program temperature set: Set point (Initial): 60 °C, Hold time (Initial): 15 min, Ramp: 15 °C/min, Set point (Final): 150 °C, Hold time (Final): 5 min. TCD temperature - 200 °C, Split ratio - 23:1.

Synthesis of Phase Pure ZIF-9 Single Crystal: In a typical synthesis process, 0.1 mmol of $Co(NO_3)_2.6H_2O$ (29.1 mg) and 0.203 mmol of Bim was dissolved into 18 mL DMF. A slight colloidal solution appeared which became clear after adding 50 µL of conc. HNO_3. The overall solution was kept at 120 °C under hydrothermal condition for 2 days. After cooling to room temperature we obtained needle like blue crystal. Single crystal diffraction analysis showed successful formation of ZIF-9 phase.

Microwave Assisted Synthesis of ZIF-9: Microwave assisted synthesis is considered as one of the sustainable approach as it requires less time and energy input. Henceforth, we have targeted to synthesis ZIF-9 nanocrystals *via* microwave assisted pathway. Briefly, 0.1 mmol of $Co(NO_3)_2.6H_2O$ (29.1 mg) and 0.203 mmol of Bim (24 mg) were dissolved in 3 mL DMF in a 10 mL G10 microwave vial. The overall solution was then mixed properly. The microwave vial was then capped and placed in a microwave reactor. The glass vial was then heated at 120 °C under stirring condition for 1 h. After cooling to room temperature (30 °C) a dark purple precipitate was obtained. The precipitate was then washed several times with DMF and H_2O and then dried at room temperature to get purple crystalline product.

Synthesis of Graphene Oxide (GO): GO was synthesized using modified Hummer's method.[1] In a typical synthesis, graphite (2 g) was reacted with 2 g of $NaNO_3$ in 90 mL H_2SO_4 under continuous stirring for 4 h in ice cold condition. After that 12 g of $KMnO_4$ was added slowly into the resulting solution at a temperature of (15-20) °C. Following this the temperature of the reaction bath was elevated slowly to 50 °C and kept for 4 h. A sudden brown coloration was observed after cooling the reaction mixture to room temperature. Then 200 mL of deionized water and 12 mL of H_2O_2 (35%) were added slowly into the abovementioned mixture. The wholesome mixture was allowed to stir for an hour and kept undisturbed for 8 h. The precipitate was washed subsequently with 1.2 (N) HCl solution and deionized water, followed by drying at room temperature (30 °C).

Microwave Assisted Synthesis of ZIF-9@xGO Composites: Briefly, x mg of GO was added in 3 mL DMF and dispersed through ultrasonication. Then, 0.1 mmol of $Co(NO_3)_2.6H_2O$ (29.1 mg) and 0.203 mmol of Bim (24 mg) were dissolved in the abovementioned dispersed solution. The overall solution was mixed thoroughly and placed in a 10 mL G10 microwave vial. The microwave vial was then capped and placed in a microwave reactor. The glass vial was then heated at 120 °C under constant stirring for 1 h. After cooling to room temperature (30 °C), we observed a deep purple precipitate. The precipitate was then washed several times with DMF and distilled water, followed by drying at room temperature to get the desired product named as ZIF-9@xGO (where x = 2.5, 5, 10 wt.% with respect to cobalt salt taken).

Electrochemical Experiment: A three-electrode system using Pt and Ag/AgCl (saturated KCl) as the counter and reference electrodes, respectively were used for the electrochemical measurements. Either 1 M KOH or 1 M KOH with 0.1 M BA was used as the electrolyte for measurements. A sample-coated glassy carbon electrode (GCE) (1.5 mm in diameter) was used as a working electrode. 0.3 and 0.05 µm alumina slurries were used to polish the GCE on a polishing pad to obtain a mirror finish, which was followed by sonication in distilled water and isopropanol successively. 2 mg of the catalyst was dispersed in a mixture of isopropanol (80 µL) and Nafion solution (5 wt %) (20 µL) and was allowed to sonicate for 30 min. 5 µL of the catalyst ink was dropped on the surface of the GCE and was dried at ambient conditions. For bulk electrocatalysis, 4 mg of the catalyst was dispersed in a mixture of isopropanol (160 µL) and Nafion solution (5 wt %) (40 µL) and was allowed to sonicate for 30 min. Prior to experiment, the nickel foam (NF) was treated with 2 M H_2SO_4 and sonicated in distilled water. The ink was dropped over 1x1 NF and was allowed to dry at ambient condition. The potential was converted to a reversible hydrogen electrode (RHE) using the Nernst equation: $E_{RHE} = E_{Ag/AgCl} + 0.059pH + 0.1976$ V at 25 °C. Cyclic voltammetry (CV) were taken at a scan rate of 10 mV s^{-1}. Electrochemical impedance spectroscopy (EIS) was carried out at 1.2 V *vs.* RHE in 1 M KOH with 0.1 M BA, with a frequency range from 0.01 Hz to 1000 kHz. A chronoamperometry test was performed at an applied potential of 1.45 V *vs.* RHE for 20000 s.

Electrochemical Benzyl Alcohol Oxidation (BAO): BAO was carried out in 1 M KOH solution containing 0.1 M BA in a three-electrode system with Pt and Ag/AgCl (saturated KCl) as the counter and reference electrodes respectively, at room temperature (30 °C). Chronoamperometry at a constant potential was carried out for 12 h. In order to analyse the product, 10 mL of the electrolyte was collected and neutralized with conc. HCl, following which it was extracted with 10 mL of ethyl acetate. The mixture was dried over anhydrous Na_2SO_4. Into the final product, 20 µL of mesitylene was added as internal standard and was analysed using ^{1}H NMR. The evolving H_2 gas was measured directly by injecting 1 mL of the gas from the headspace of the electrolytic cell into CS-5800D Centurion Scientific GC (TCD detector) by bubbling Argon at a rate of 8.85 mL min^{-1}.

The benzyl alcohol (BA) conversion, benzoic acid selectivity, and yield were calculated following the equations:[2]

$$\text{BA conversion (\%)} = \frac{initial\ concentration\ of\ BA - final\ concentration\ of\ BA\ remaining}{initial\ concentration\ of\ BA} \text{ x } 100\%$$

$$\text{Benzoic acid selectivity (\%)} = \frac{Concentration\ of\ benzoic\ acid\ formed}{Concentration\ of\ BA\ converted} \text{ x } 100\%$$

$$\text{Benzoic acid yield (\%)} = \frac{BA\ conversion\ (\%) \times Benzoic\ acid\ selectivity\ (\%)}{100}$$

The Faradic efficiency (FE) was calculated by using the following equation:

$$\text{FE\%} = \frac{n \times F \times mol\ of\ (PhCHO\ or\ PhCOOH)}{Q}$$

Where, n is the number of electrons involved (*i.e.*, 2 for PhCHO and 4 for PhCOOH), F is the Faraday constant (96,485 C mol^{-1}), Q is the total charge passed.

Table S1. Crystal and Structure Refinement Data of ZIF-9.

Empirical formula	$C_{3.82}\ H_{2.73}\ Co_{0.27}\ N_{1.09}$
Colour	Violet
Cell_measurement temperature	145.34 K
Formula Weight	79.96
Radiation Wavelength	0.71073 Å
Crystal System, Space Group	Trigonal, *R* -3
Unit Cell Dimensions	a = 22.7932(15) Å, b = 22.7932(15) Å, c = 15.838(3) Å and α = 90º, β = 90º, γ = 120º
Cell Volume	7126.1
Z, Calculated density	66, 1.230
Absorption Coefficient	1.075
***F*(000)**	2682
Theta range	2.771 to 24.990
Limiting indices	-27≤ h ≥27, -27≤ k ≥27, -18≤ l ≥18
Max. and Min. Transmission	0.807 and 0.686
Refinement Method	Full-matrix least-squares on F^2
Goodness-of-fit on F^2	1.088
R factor (%)	2.73

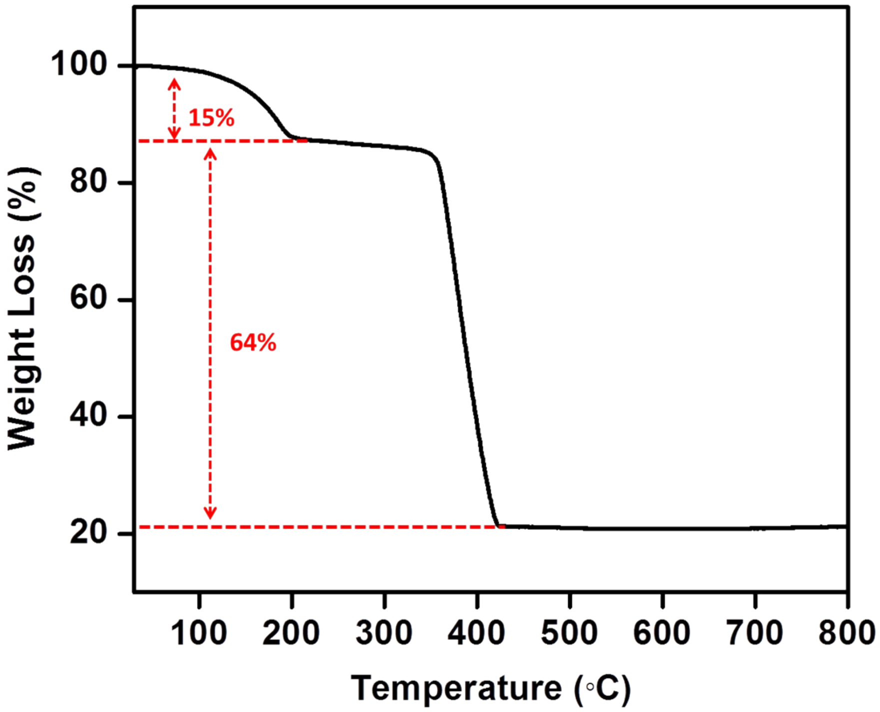

Figure S1. TGA curve of ZIF-9.

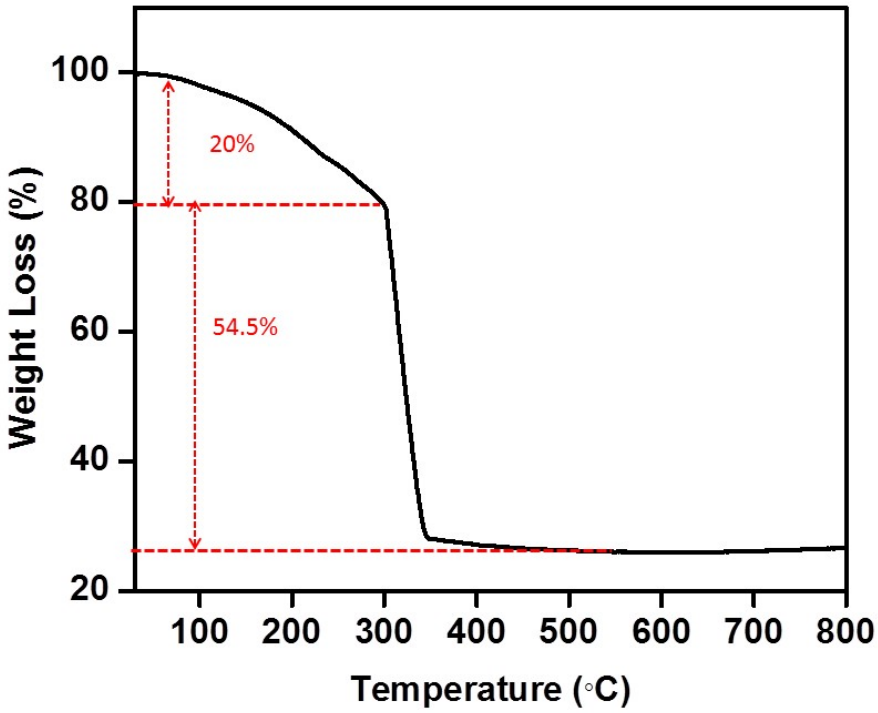

Figure S2. TGA curve of ZIF-9@10GO.

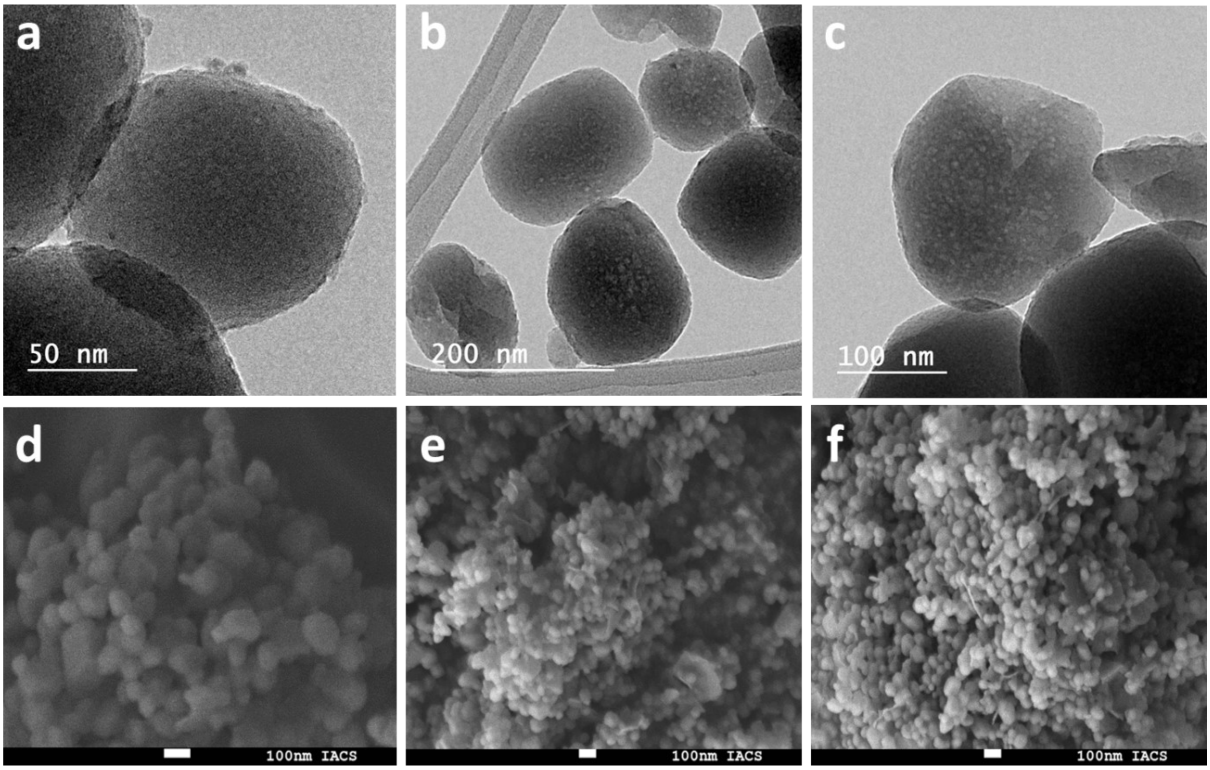

Figure S3. HRTEM images of a) ZIF-9; b) ZIF-9@2.5GO and c) ZIF-9@5GO. FESEM images of d) ZIF-9; e) ZIF-9@2.5GO and f) ZIF-9@5GO.

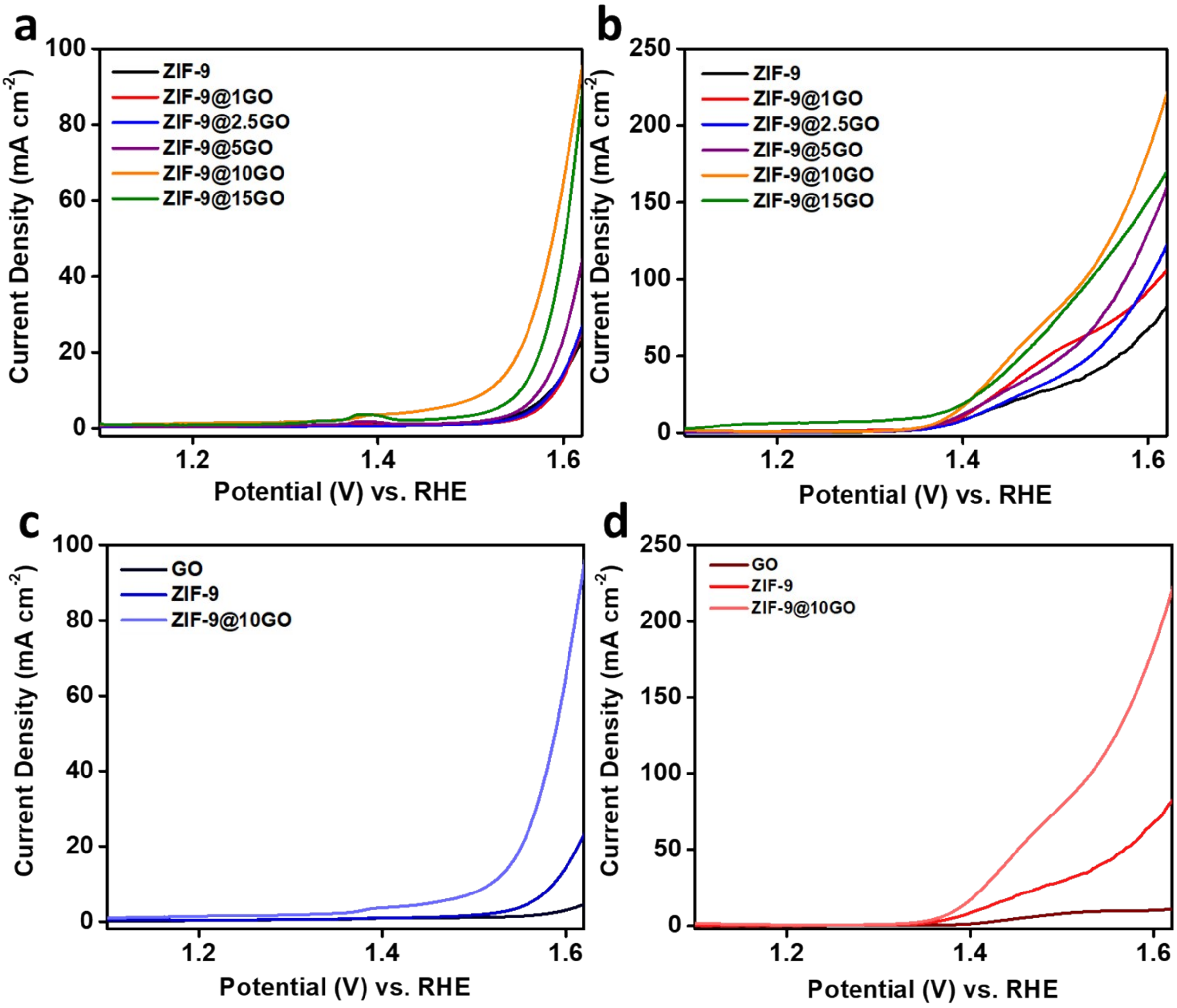

Figure S4. LSV curves of ZIF-9 (black), ZIF-9@1GO (red), ZIF-9@2.5GO (blue), ZIF-9@5GO (purple), ZIF-9@10GO (orange) and ZIF-9@15GO (green) in a) 1 M KOH and b) 1 M KOH with 0.1 M BA. LSV curves comparing the activity of GO with ZIF-9 and ZIF-9@10GO in c) 1 M KOH and d) 1 M KOH with 0.1 M BA.

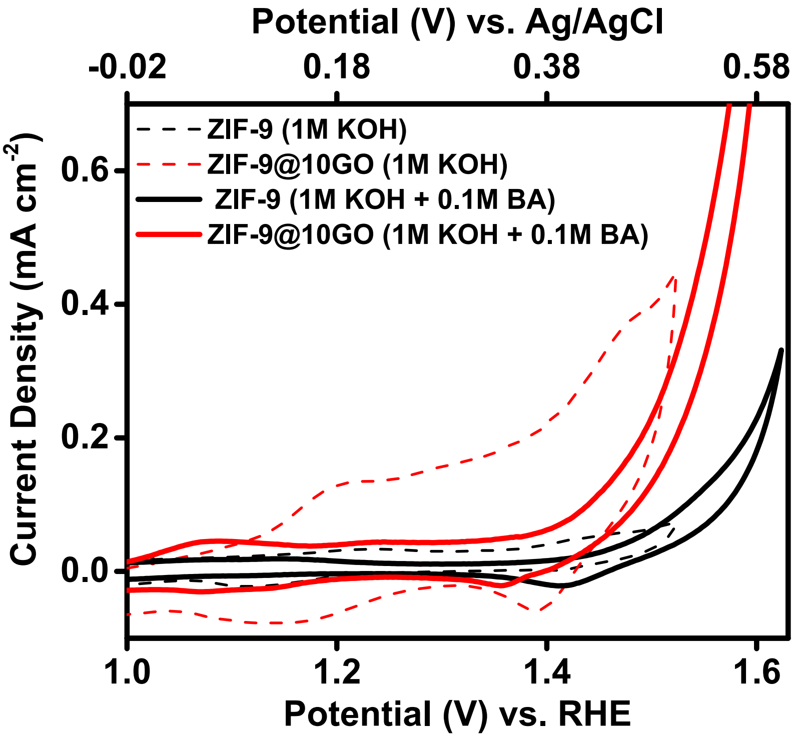

Figure S5. CV curves of ZIF-9 (black) and ZIF-9@10GO (red) in 1 M KOH (dotted line) and 1 M KOH with 0.1 M BA (bold line).

Table S2. R_s and R_{ct} values of the electrocatalysts in 1 M KOH + 0.1 M BA.

Electrocatalyst	**R_s (Ω.cm^2)**	**R_{ct} (Ω.cm^2)**
ZIF-9@10GO	0.2169	380.7
ZIF-9@5GO	0.3681	540.9
ZIF-9@2.5GO	0.4167	629.1
ZIF-9	0.4896	768.6

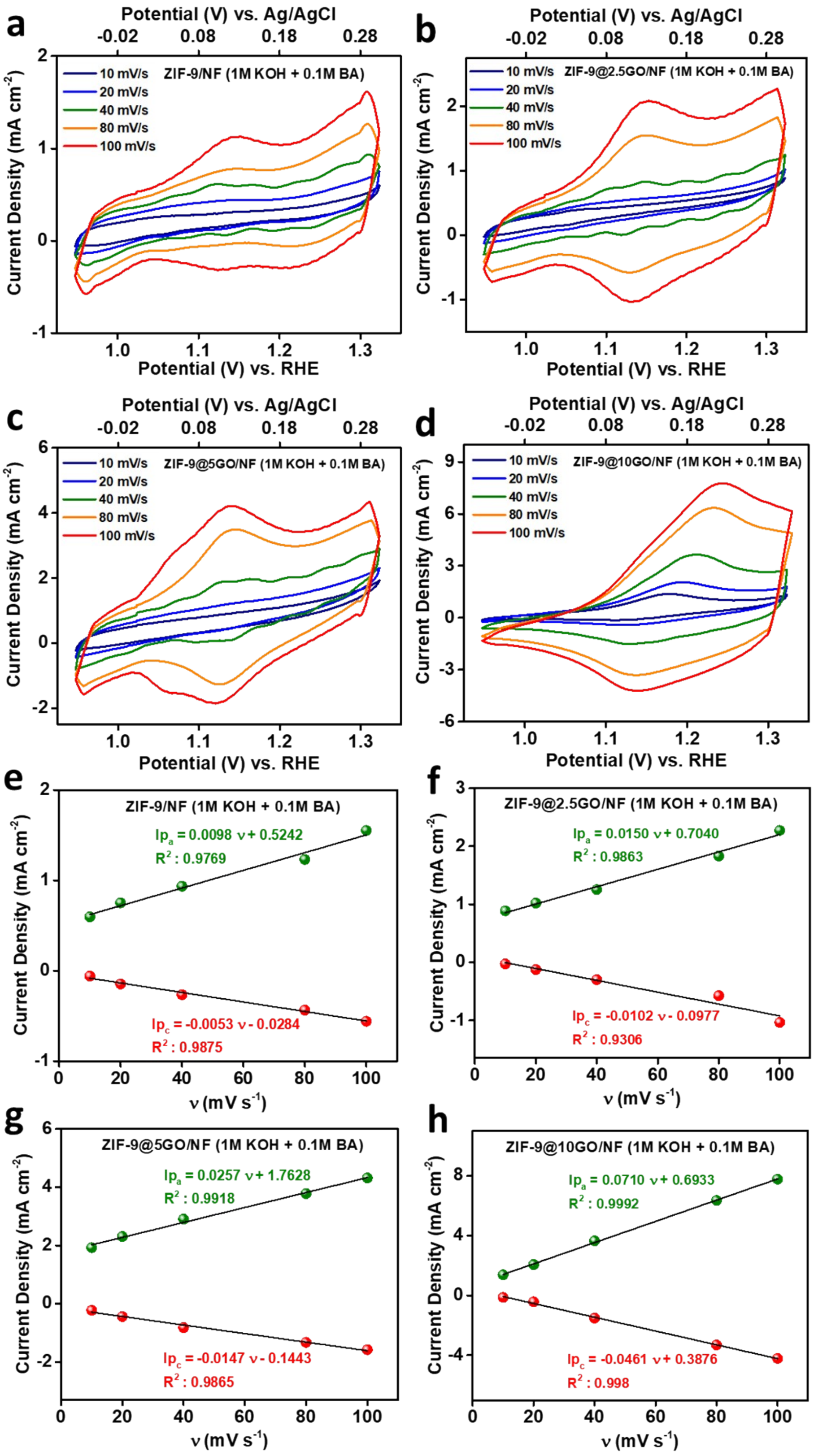

Figure S6. (a-d) CV curves of ZIF-9, ZIF-9@2.5GO, ZIF-9@5GO and ZIF-9@10GO in 1 M KOH with 0.1 M BA over NF at different scan rates. (e-h) Relationship between anodic and cathodic peak current densities with scan rates.

Table S3. Surface coverage of the electrocatalysts in 1 M KOH + 0.1 M BA.

Electrocatalyst	Surface Coverage (Γ) (mol cm^{-2})
ZIF-9	8.03×10^{-9}
ZIF-9@2.5GO	1.34×10^{-8}
ZIF-9@5GO	2.15×10^{-8}
ZIF-9@10GO	6.23×10^{-8}

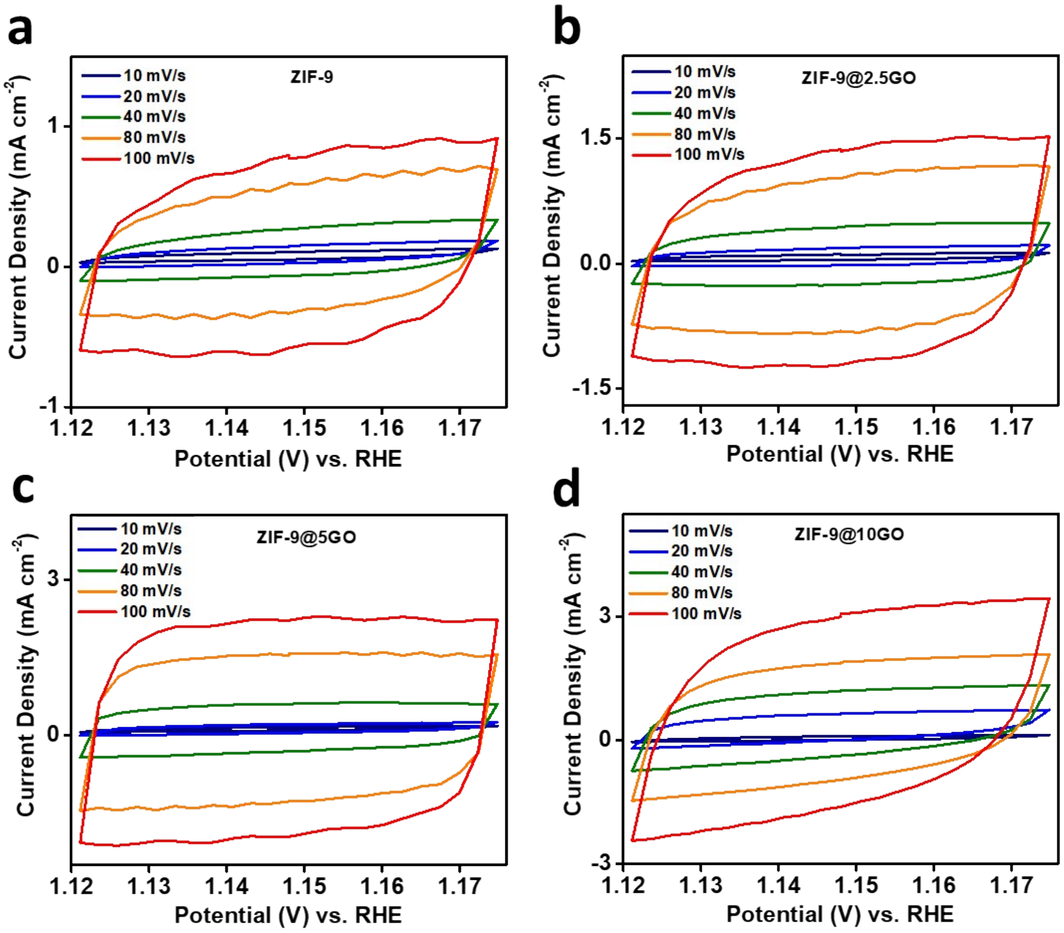

Figure S7. (a-d) ECSA determined by CV at non-faradic region for the electrocatalysts in 1 M KOH with 0.1 M BA.

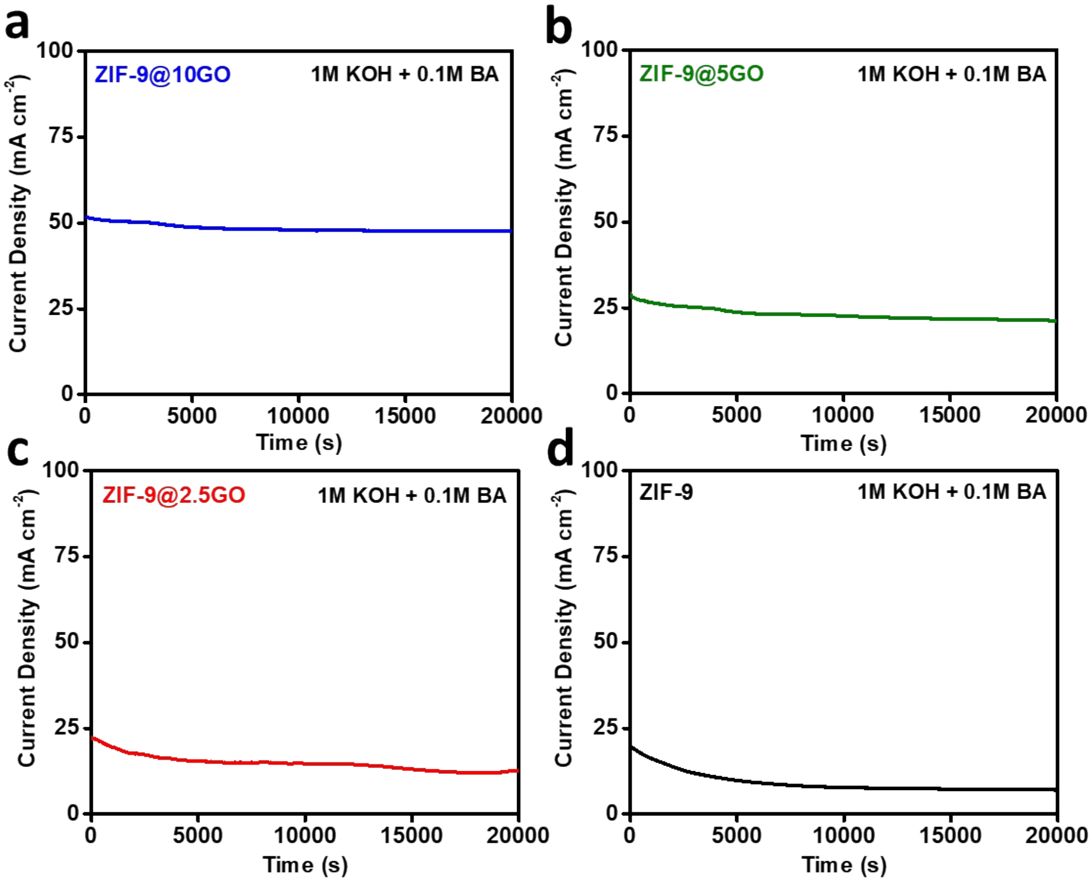

Figure S8. Chronoamperometric measurements of (a) ZIF-9@10GO, (b) ZIF-9@5GO, (c) ZIF-9@2.5GO and (d) ZIF-9 over NF using a constant potential of 1.45 V vs. RHE in a 1 M KOH with 0.1 M BA.

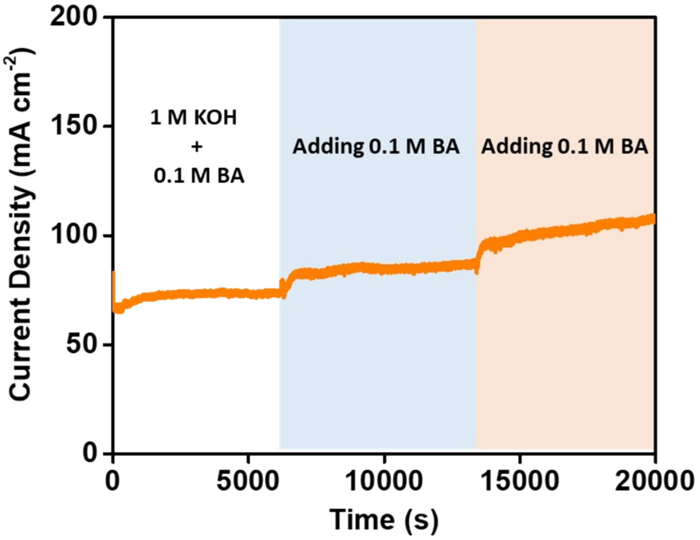

Figure S9. Chronoamperometric response with each addition of 0.1 M BA over ZIF-9@10GO/NF at a constant potential of 1.45 V *vs.* RHE.

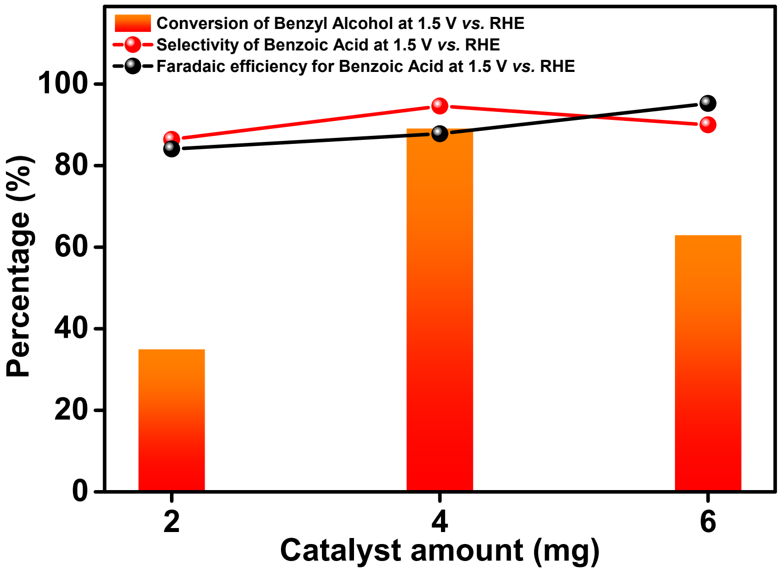

Figure S10. Effect of ZIF-9@10GO electrocatalyst mass loading over (1×1) NF on the BA oxidation at 1.50 V *vs.* RHE in 1 M KOH.

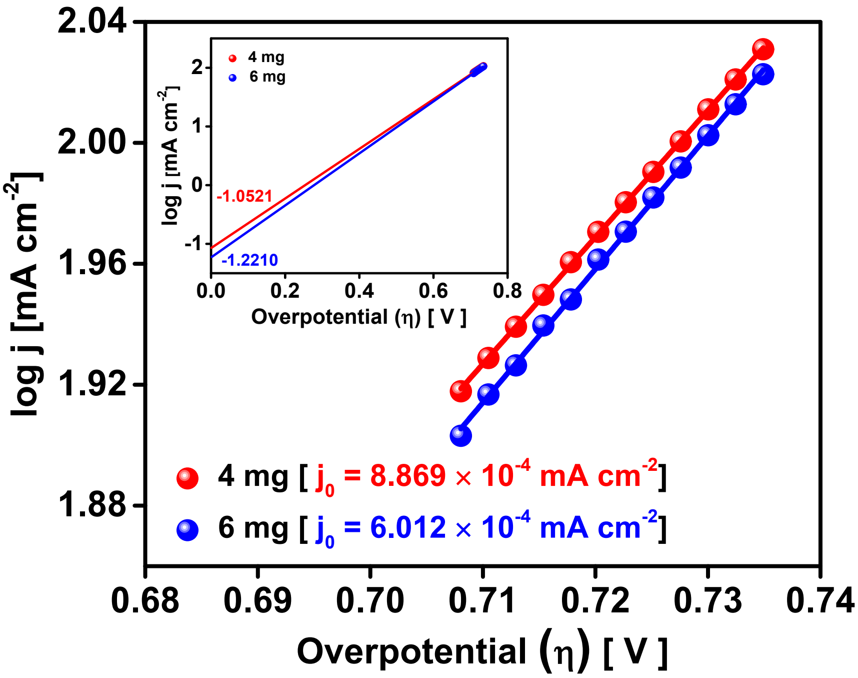

Figure S11. log j *vs*. overpotential plot (Inset: extrapolation of the Tafel line).

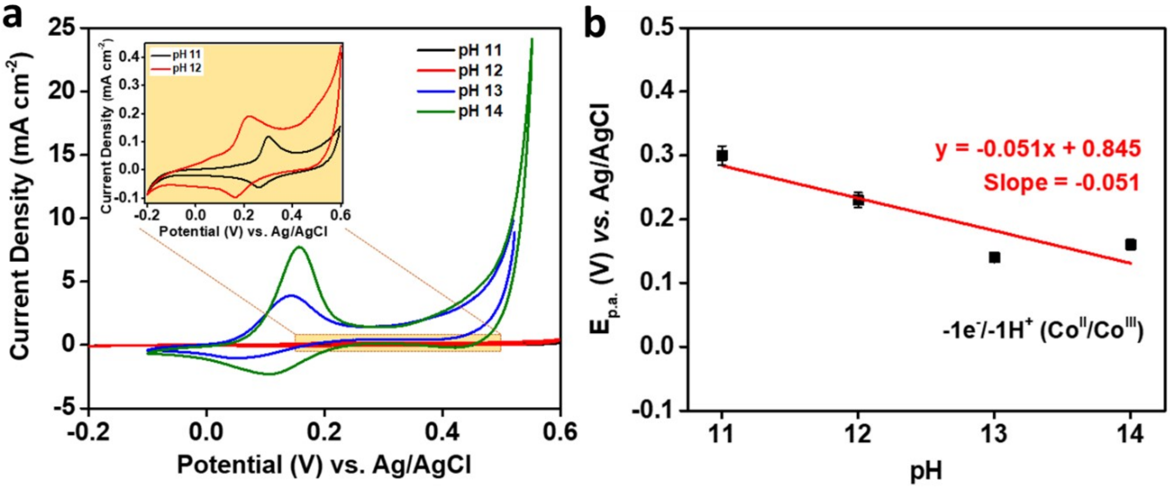

Figure S12. a) Cyclic voltammetry of ZIF-9@10GO at different pH in presence of 0.1 M BA. b) Pourbaix diagram of the redox active species.

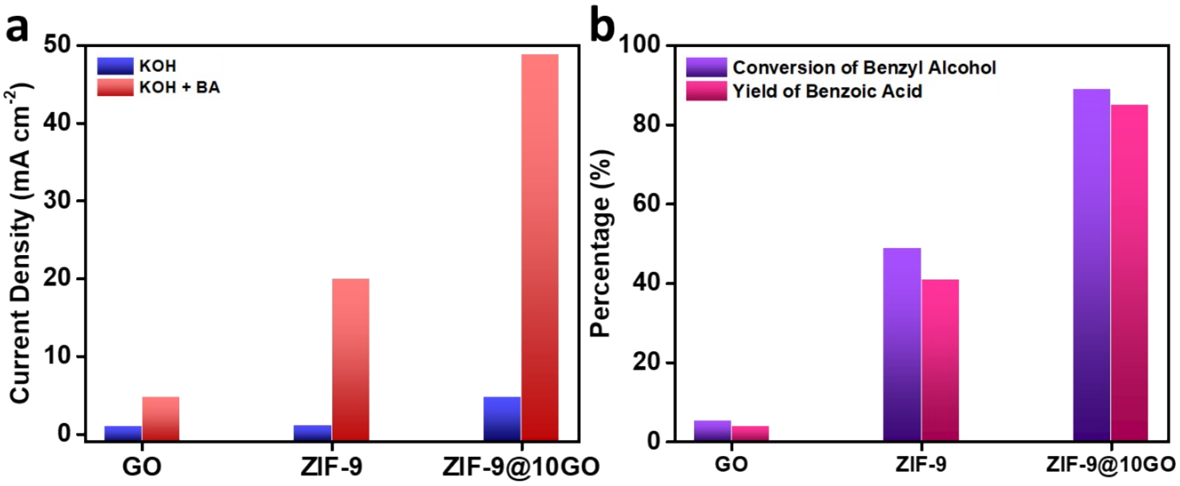

Figure S13. a) Current density obtained by GO, ZIF-9 and ZIF-9@10GO loaded over NF in 1 M KOH and 1 M KOH with 0.1 M BA. b) Catalytic activity of GO, ZIF-9 and ZIF-9@10GO.

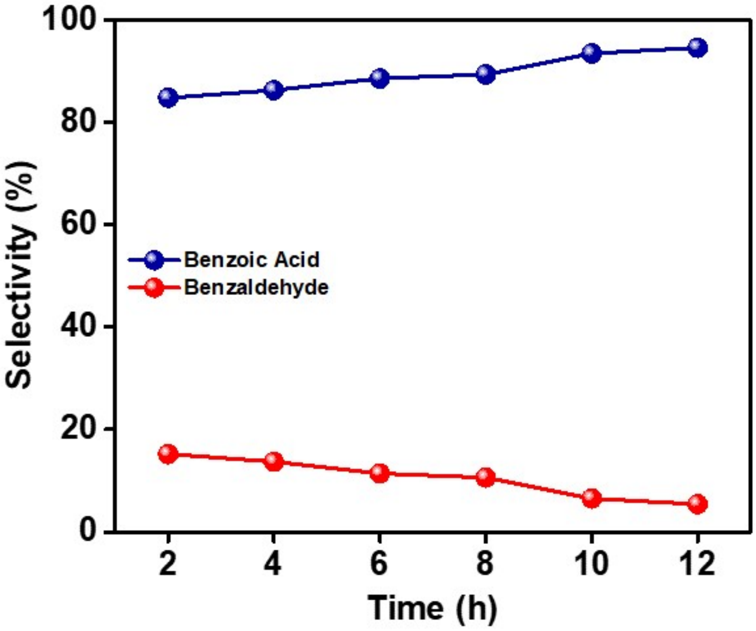

Figure S14. Benzoic acid selectivity *vs*. time plot at constant potential of 1.50 V *vs*. RHE.

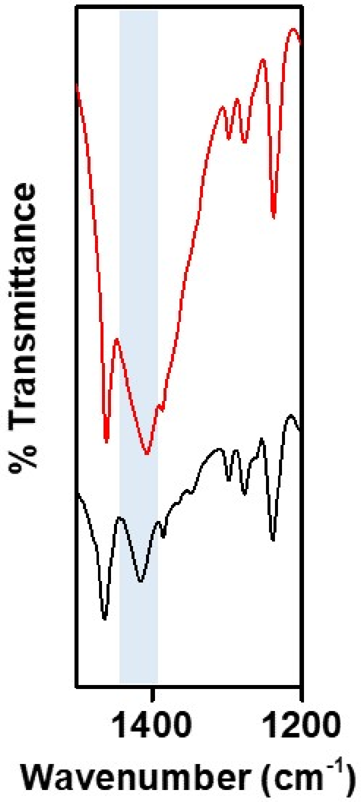

Figure S15. FTIR spectra of ZIF-9@10GO after electrochemical oxidation; red – without heat treatment, black – after heat treatment at 100 °C.

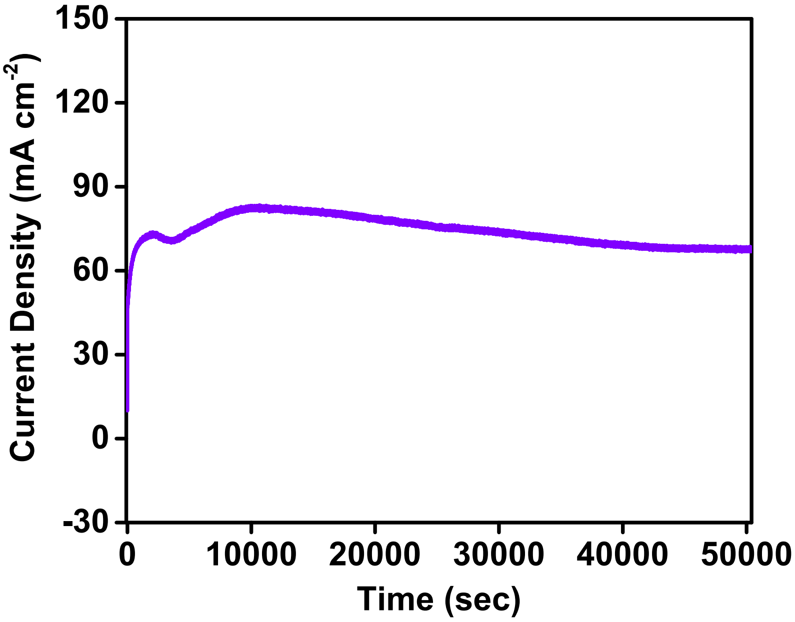

Figure S16. Chronoamperometric measurements of ZIF-9@10GO/NF for 12 h under a constant potential of 1.5 V *vs*. RHE in 1 M KOH with 0.1 M BA.

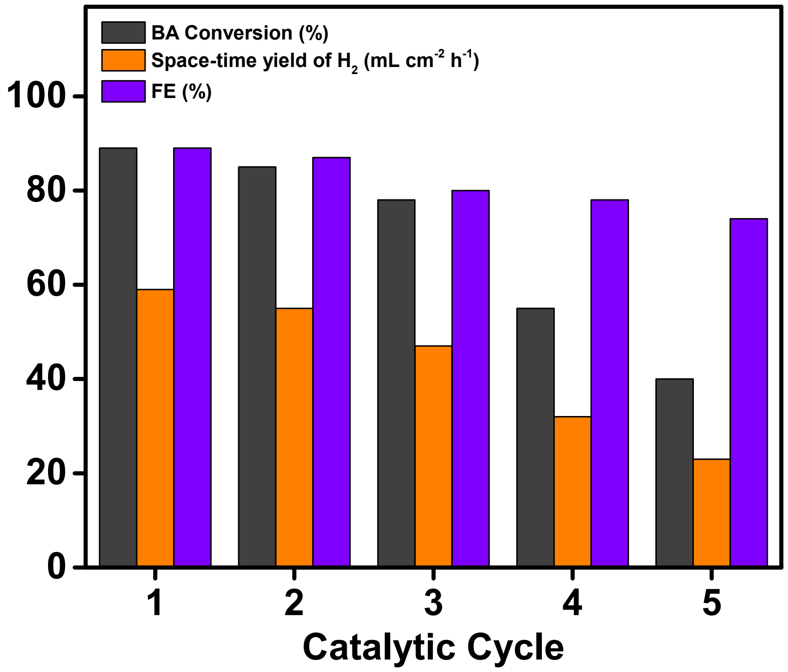

Figure S17. Benzyl alcohol conversion, space-time rate of yield of H_2 and faradaic efficiency under five successive catalytic cycles using ZIF-9@10GO/NF catalyst at 1.5 V *vs*. RHE in 1 M KOH solution.

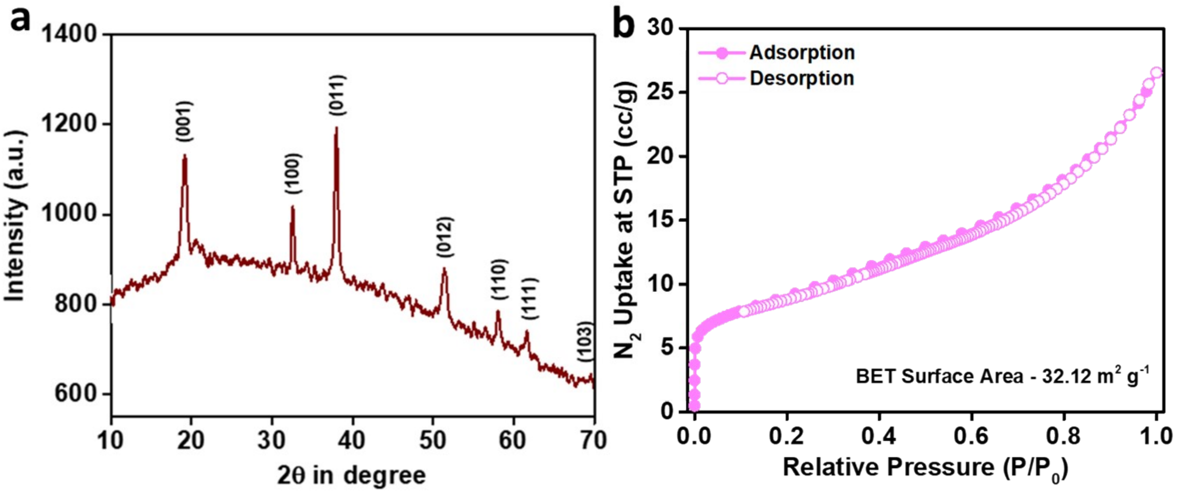

Figure S18. a) PXRD pattern of β-Co(OH)$_2$, b) N_2 sorption plot of β-Co(OH)$_2$.

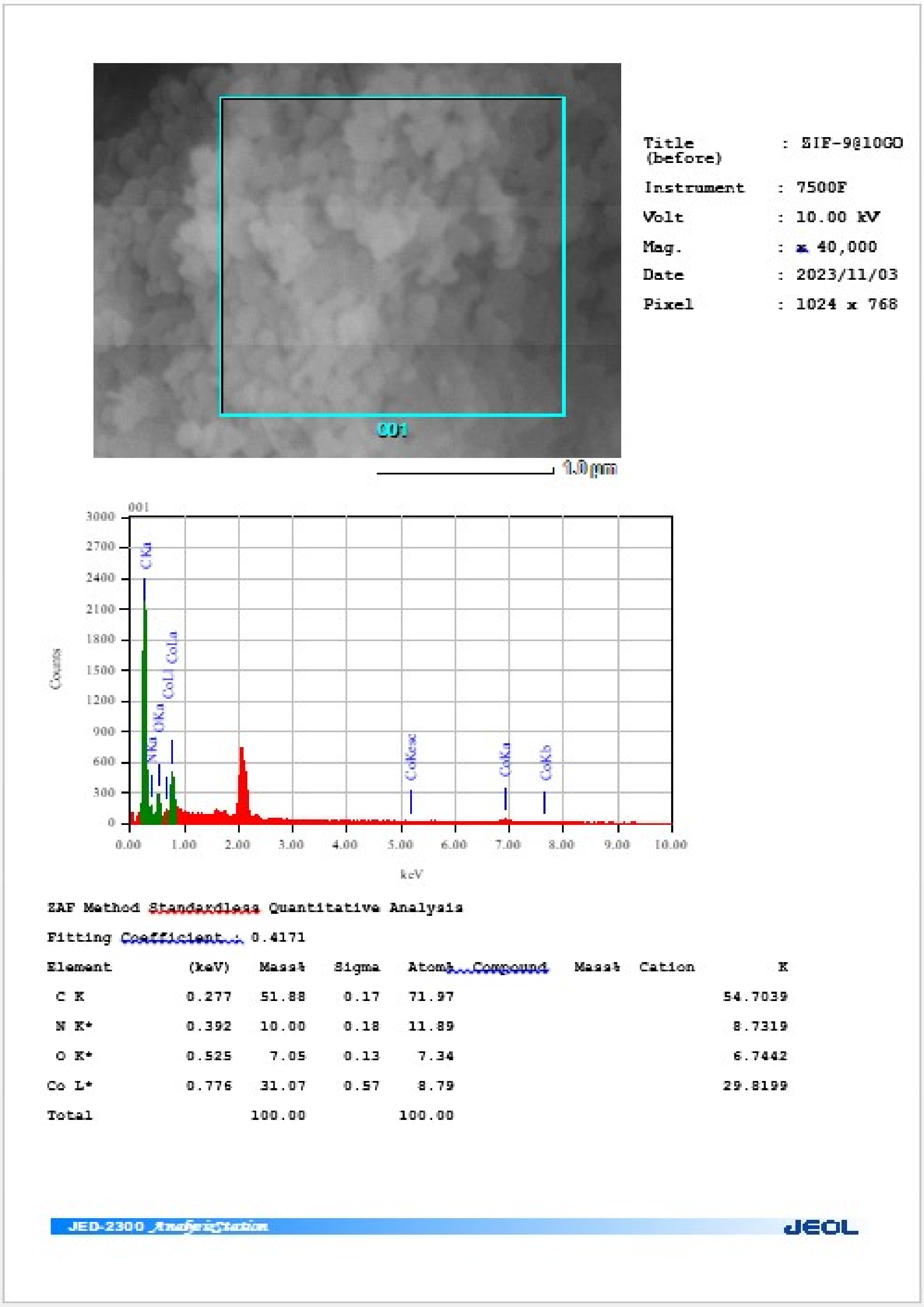

Title : ZIF-9@10GO
(before)
Instrument : 7500F
Volt : 10.00 kV
Mag. : x 40,000
Date : 2023/11/03
Pixel : 1024 x 768

ZAF Method Standardless Quantitative Analysis

Fitting Coefficient : 0.4171

Element	(keV)	Mass%	Sigma	Atom%	Compound	Mass%	Cation	K
C K	0.277	51.88	0.17	71.97				54.7039
N K*	0.392	10.00	0.18	11.89				8.7319
O K*	0.525	7.05	0.13	7.34				6.7442
Co L*	0.776	31.07	0.57	8.79				29.8199
Total		100.00		100.00				

Figure S19. EDX spectra of ZIF-9@10GO before electrocatalysis.

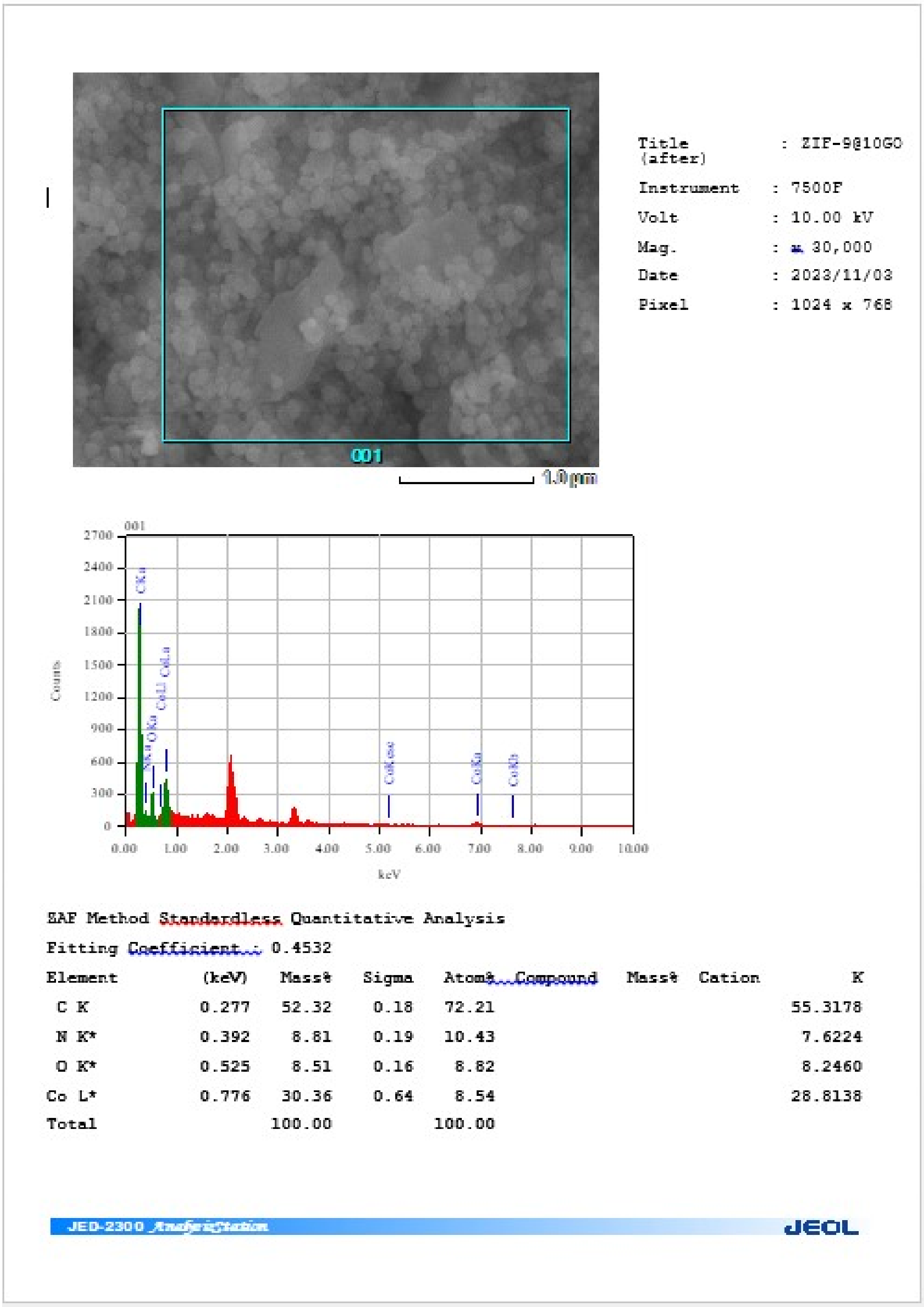

Title : ZIF-9@10GO (after)
Instrument : 7500F
Volt : 10.00 kV
Mag. : x 30,000
Date : 2023/11/03
Pixel : 1024 x 768

ZAF Method Standardless Quantitative Analysis

Fitting Coefficient : 0.4532

Element	(keV)	Mass%	Sigma	Atom%	Compound	Mass%	Cation	K
C K	0.277	52.32	0.18	72.21				55.3178
N K*	0.392	8.81	0.19	10.43				7.6224
O K*	0.525	8.51	0.16	8.82				8.2460
Co L*	0.776	30.36	0.64	8.54				28.8138
Total		100.00		100.00				

Figure S20. EDX spectra of ZIF-9@10GO after electrocatalysis.

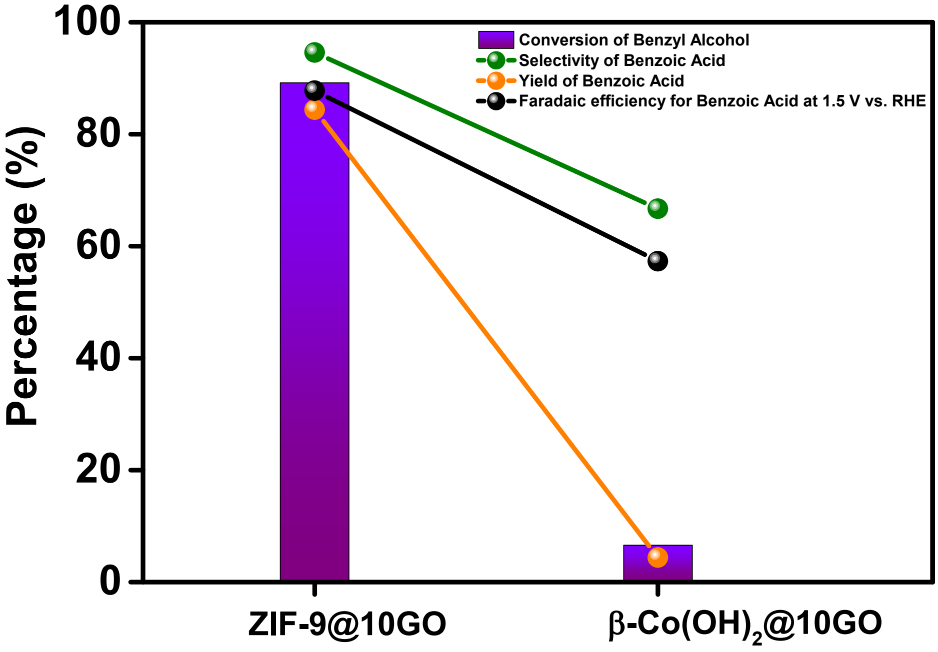

Figure S21. Comparison of the catalytic performance between ZIF-9@10GO and β-Co(OH)$_2$@10GO.

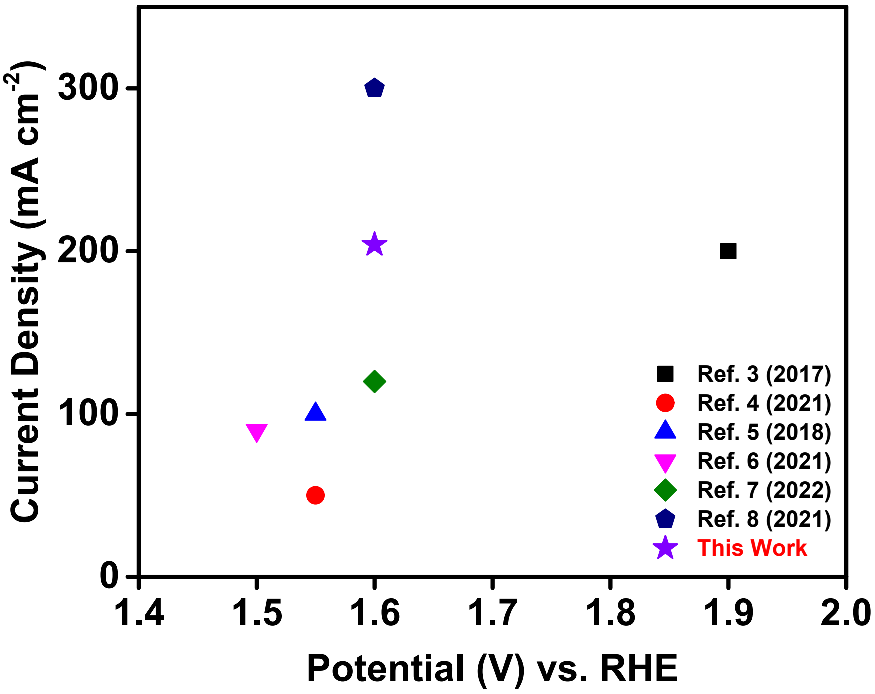

Figure S22. Current densities obtained from the anodic oxidation reactions reported in the literatures over various non-noble based electrocatalysts and our ZIF-9@10GO.

Table S4. Comparison table of catalytic performance for the coupled H_2 production.

Sl. No.	**Catalyst**	**Experiment**	**Reactant at Anode**	**Coupled H_2 Production Rate ($mmol \cdot g^{-1} \cdot h^{-1}$)**	**References**
1.	$PW_{10}Cu_2$@CMC	Electrocatalytic	S-N/S-S coupling	0.05	*Adv. Mater.* **2023**, 2304716.
2.	Cu_3Ag_7	Electrocatalytic	Formaldehyde	5.95[a]	*Nat. Commun.* **2023**, *14*, 525.
3.	Ru/MPNC	Electrocatalytic	Hydrazine	0.893[a]	*Nano Energy* **2022**, *100*, 107467
4.	Ni-Modified CdS	Photocatalytic	2-Propanol	46.6	*J. Am. Chem. Soc.* **2016**, *138,* 10128-10131.
5.	CoNiP	Electrocatalytic	5-HMF	91.9	*Appl. Catal. B: Environ.* **2022**, *312*, 121400.
6.	NiCo/MXene	Electrocatalytic	Hydrazine	9200	*Nat. Commun.* **2021**, *12*, 4182.
7.	ZIF-9@10GO	Electrocatalytic	Benzyl alcohol	273	This Work

[a] $mmol \cdot h^{-1}$

References

1. J. Jo, S. Lee, J. Gim, J. Song, S. Kim, V. Mathew, M. H. Alfaruqi, S. Kim, J. Lim and J. Kim, *R. Soc. Open Sci*. 2019, **6**, 181978.

2. Y. Jiang, Y. Liu, Y. He and D. Li, *ACS Catal.* 2022, **12**, 14140-14151.

3. J. Zheng, X. Chen, X. Zhong, S. Li, T. Liu, G. Zhuang, X. Li, S. Deng, D. Mei and J. G. Wang, *Adv. Funct. Mater.* 2017, **27**, 1704169.

4. L. Ming, X. Y. Wu, S. S. Wang, W. Wu and C. Z. Lu, *Green Chem.* 2021, **23**, 7825-7830.

5. Y. Huang, R. Yang, G. Anandhababu, J. Xie, J. Lv, X. Zhao, X. Wang, M. Wu and Q. Li, *ACS Energy Lett*. 2018, **3**, 1854-1860.

6. Y. Cao, D. Zhang, X. Kong, F. Zhang and X. Lei, *J. Mater. Sci*. 2021, **56**, 6689-6703.

7. N. Shilpa, A. Pandikassala, P. Krishnaraj, P. S. Walko, R. N. Devi and S. Kurungot, *ACS Appl. Mater. Interfaces* 2022, **14**, 16222-16232.

8. P. Hao, R. Xu, Q. Wang, Z. Zhao, H. Wen, J. Xie, F. Lei, G. Cui and B. Tang, *Chem. Commun.* 2021, **57**, 13752-13755.